Biocatalysis and Agricultural Biotechnology 20 (2019) 101187

Contents lists available at ScienceDirect

Biocatalysis and Agricultural Biotechnology

journal homepage: www.elsevier.com/locate/bab

Process optimization of solvent extraction of seed oil from *Moringa oleifera*: An appraisal of quantitative and qualitative process variables on oil quality using D-optimal design

Babatunde Oladipo, Eriola Betiku*

Biochemical Engineering Laboratory, Department of Chemical Engineering, Obafemi Awolowo University, Ile-Ife, 220005, Osun State, Nigeria

ARTICLE INFO

Keywords:
Vegetable oil
Solvent extraction
Moringa oleifera
Modeling
Optimization

ABSTRACT

Moringa oleifera seed oil (MOSO) was extracted from its kernels using solvent extraction method. The effect of extraction time (1–3 h), solid/solvent ratio (0.050–0.200 g/ml) and type of solvent (ethyl acetate, ethanol and *n*-hexane) on MOSO yield were assessed. The coefficient of determination - R^2, adjusted R^2, and predicted R^2 of 0.9993, 0.9986 and 0.9965, respectively obtained demonstrate the model developed can effectively explain the extraction processts. Optimal condition of extraction time of 3 h, solid/solvent ratio of 0.050 g/ml and *n*-hexane established for the process could be used to obtain MOSO yield of 41.72 ± 0.45 wt%. Extraction efficacy test showed ethanol, ethyl acetate and *n*-hexane gave maximum MOSO yield of 8.24 ± 0.00, 14.28 ± 0.22 and 42.00 ± 0.45 wt%, respectively. The physical and chemical properties of the MOSO differed on the basis of choice of solvent used for the extraction. The acid values of the oil were 8.25 ± 0.01, 3.40 ± 0.04 and 2.88 ± 0.07 mg KOH/g oil with ethanol, ethyl acetate and *n*-hexane. Fatty acid profile analysis of the MOSO samples confirms that a high-oleic oil could be produced from *Moringa oleifera* seeds, and thus, could potentially serve as feedstock for chemical and food processing industries.

1. Introduction

Attention of researchers has been stimulated on the application of plant oils as raw material for food and industrial purposes. Therefore, identification, characterization, development, utilization and cost-effective production techniques of such beneficial vegetable oils, have been on the increase. To meet the global needs on food due to the rising world population, it has become imperative to take advantage of more vegetable oils.

Moringa oleifera is a member of the genus Moringaceae. It is a high-valued plant that is versatile, adaptable, easy to cultivate and self-propagating with fast growth rate. It is grown across Nigeria and it is known in local languages as *ewe igbale*, *idagbomunonye* and *zogelle*. Different uses of *Moringa* oil has been reported such as in frying applications (Abdulkarim et al., 2007), biodiesel production (Rashid et al., 2011), anticancer activities (Elsayed et al., 2015) and cosmetic products (Mahmood et al., 2010).

Techniques utilized for oil extraction could alter small components which have functional properties and contribute to oxidation stability. Numerous methods namely; traditional or mechanical method (Bargale et al., 1999), aqueous enzymatic oil extraction (Latif and Anwar, 2011), solvent extraction via Soxhlet apparatus (Okeleye and Betiku, 2019), microwave-aided extraction (Taghvaei et al., 2014; Ibrahim et al., 2019), ultrasonic-aided extraction (Tian et al., 2013), pressurized solvent extraction (Dunford and Zhang, 2003) and supercritical fluid extraction (Pradhan et al., 2010) have all been investigated in oil extraction from numerous plant seeds. Among these methods, solvent extraction has been widely embraced because it is economical and simple to use. It has ability to allow for several extractions to be carried out in parallel and produce high efficiency in oil recovery. Its effectiveness hinge on extraction temperature, residence time, seed particle size, seed pretreatment conditions, solvent type and nature of oil (Mani et al., 2007).

Selection of solvent used for oil extraction also plays essential role in influencing product quality. Various researches have been carried out on the impact of polarity of solvents on characteristics of several vegetable oils. Polar solvents such as ethanol (Bhatnagar and Krishna, 2013), acetone (Okeleye and Betiku, 2019) and ethyl acetate (Lohani et al., 2015); and non-polar solvents such as *n*-hexane (Akintunde et al., 2015), petroleum ether (Kittiphoom and Sutasinee, 2013) and chloroform (Bhatnagar and Krishna, 2013), have all been investigated in oil extraction studies from several plant seeds.

---

* Corresponding author.
E-mail address: ebetiku@oauife.edu.ng (E. Betiku).

https://doi.org/10.1016/j.bcab.2019.101187
Received 21 March 2019; Received in revised form 27 May 2019; Accepted 29 May 2019

Abbreviations

ANOVA	analysis of variance
AV	acid value
BAPE	bis-allylic position equivalents
BBD	Box–Behnken design
CCD	central composite design
CV	coefficient of variation
DF	degree of freedom
FFA	free fatty acid
FT-IR	Fourier transform infrared
GC	gas chromatography
MOSO	*Moringa oleifera* seed oil
OSI	oxidative stability index
PRESS	predicted residual error sum of squares
PV	peroxide value
R^2	coefficient of determination
RSM	response surface methodology
SD	standard deviation
SS	sum of squares

Literature search revealed small information on modeling and optimization of oil extraction from *Moringa* seed. In the work reported by Abdulkareem and colleagues in which factorial design was applied, highest *Moringa* oil yield of 43.01 wt% was obtained using process condition of particle size of 500 µm, extraction time of 7 h and temperature of 65 °C with *n*-hexane (Abdulkareem et al., 2011). In the studies of *Moringa* oil extraction optimization via response surface methodology (RSM), Mani et al. (2007) assessed performance of acetone, petroleum ether and *n*-hexane, and observed 30.33, 29.98 and 33.47 wt% oil yield using residence time of 6.75, 9.47 and 7.09 h, respectively. Besides the longer extraction time which may result into high cost of energy associated, the quality characterization of the oil was not reported making it impossible to see the effect of the solvents. Other studies have been reported on the quality and yield of *Moringa* oil extracted via solvent extraction (Anwar and Bhanger, 2003; Rahman et al., 2009; Zhong et al., 2018). However, these studies were not modeled and optimized. These gaps need to be addressed in a single study.

RSM is an assembly of mathematical and statistical procedures beneficial for developing, refining and optimizing processes (Myers et al., 2009). Process optimization of oil extraction from various oilseeds using RSM combined with either central composite design (CCD) or Box–Behnken design (BBD) or D-optimal design have been reported (Mani et al., 2007; Akintunde et al., 2015). One of the benefits of D-optimal design is its ability to minimize variance of regression coefficients. It also produces very flat fraction of design space curves for most of the design space, which makes it more desirable for prediction performance (Myers et al., 2009). Unlike BBD and CCD which only allow quantitative variables, both quantitative and qualitative variables can be included in the experimental design with D-optimal design method (Akintunde et al., 2015; Okeleye and Betiku, 2019).

Thus, this present investigation aimed at modeling and optimization of the process of solvent extraction of *Moringa oleifera* seed oil (MOSO). The D-optimal design was employed to examine the effect of the regressor (independent) variables: solid/solvent ratio and extraction time (quantitative process variables) and solvent type (qualitative process variable) together with their interactions on the MOSO yield. Besides, process variables optimization was carried out using RSM. Quality characterization was carried out to ascertain the influence of solvents of extraction on the physical and chemical properties, fatty acid profiles and functional groups of the oil to determine its potential exploitation in food and chemical industries.

2. Materials and methods

2.1. Materials

2.1.1. M. oleifera seeds and chemicals

Mature *Moringa* fruit employed in this work was procured from Oja Ife market in Ile-Ife, which is situated at a longitude of 4.5667° E and latitude of 7.4667° N, southwestern Nigeria. Reagents and chemicals used in this work include Wij's solution, cyclohexane, diethyl ether, *n*-hexane, ethanol, methanol, sulfuric acid, phenolphthalein, potassium hydroxide, potassium chloride and hydrogen chloride. The reagents and chemicals were of analytical grade manufactured by J.T. Baker (USA), GFS Chemicals Inc. (USA) and BDH Chemicals Ltd., Poole England.

2.2. Methods

2.2.1. Preparation of kernels

Mature seeds enclosed in a fairly light wooded shells with three papery wings were removed by hand from their dried brown pods. The seeds were manually dehulled from the shells to get the kernels and then sorted. Undamaged kernels were selected and oven-dried at 103 °C for 3 h to attain uniform weight. Dried kernels were finely pulverized using a blending machine and was kept in corked bottles under cool-dry storage condition for further use.

2.2.2. D-optimal design and modeling

D-optimal method of design was used for the extraction studies (Akintunde et al., 2015; Okeleye and Betiku, 2019). The design used in this present work had two quantitative variables (solid/solvent ratio and extraction time) and a qualitative variable (solvent type) designated as *A*, *B* and *C*, respectively (Table 1). The experimental design produced 24 experiments, specifying 12 required model points, 6 lack-of-fit points and 6 replicate points. The replicate runs minimize the effect of unusual observations or outliers that may occur at the design points. It also gives room for an estimate of error to be made and for checking model accuracy.

For statistical calculations, the test factors were coded in the regression equation based on the expression in Eq. (1):

$$Z_i = \frac{U_i - U_j}{\Delta U_i}; \quad i = 1,\ 2,\ 3 \tag{1}$$

where, Z_i represents coded value of regressor variable, U_i represents real value of regressor variable, U_j represents real value of regressor variable U_i at the center point and ΔU_i represents the step change in U_i. Hence, the regressor variables ranged from −1 to +1 for the appraisal of factors.

The relationship between the response variable which depends on the regressor variables for the process, is depicted by the polynomial model in Eq. (2):

$$\widehat{Y} = \mu_o + \mu_1 A + \mu_2 B + \mu_3 C + \mu_{12} AB + \mu_{13} AC + \mu_{23} BC + \mu_{11} A^2 + \mu_{22} B^2 + \mu_{33} C^2 \tag{2}$$

where, $\hat{Y}$ is the predicted MOSO yield (response), μ_0 is the intercept

Table 1
Factors considered for extraction process using D-optimal design.

Factor	Unit	Type	Coded factor levels		
			−1	0	+1
Solid/solvent ratio (A)	g/ml	Quantitative	0.050	0.125	0.200
Extraction time (B)	h	Quantitative	1	1.5	3
Solvent type (C)	–	Qualitative	*n*-hexane	ethyl acetate	ethanol

term, μ_1, μ_2 and μ_3 are the partial regression coefficients, μ_{12}, μ_{13} and μ_{23} are the interaction regression coefficients, μ_{11}, μ_{22} and μ_{33} are the quadratic regression coefficients, and A, B and C are the coded regressor variables representing solid/solvent ratio, extraction time and solvent type, respectively.

The fitted polynomial equation is presented as contour and surface plots in order to visualize the association between the response and observed levels of each variable and infer the maximum conditions. To know the breakdown of the total variability in the response variable, analysis of variance (ANOVA) was done to calculate the lack-of-fit and to identify the impact of the model terms on MOSO yield. Coefficient of determination (R^2), adjusted R^2 and predicted R^2 in Eqs. (3)–(5), respectively, were used to appraise the quality of fit of the polynomial model (Myers et al., 2009). The standard deviation (*SD*), coefficient of variation (*CV*) and adequate precision ratio in Eqs. (6)–(8), respectively (Myers et al., 2009), and also the p-value and F-value were employed to check the statistical significance.

$$R^2 = 1 - \frac{SS_{residual}}{SS_{model} + SS_{residual}} \tag{3}$$

$$\text{Adjusted } R^2 = 1 - \frac{SS_{residual}/DF_{residual}}{(SS_{model} + SS_{residual})/(DF_{model} + DF_{residual})} \tag{4}$$

$$\text{Predicted } R^2 = 1 - \frac{PRESS}{SS_{total} - SS_{block}} \tag{5}$$

$$SD = \sqrt{MS_e} \tag{6}$$

$$CV = \frac{\sqrt{MS_e}}{\frac{1}{n}\sum_1^n Y} \times 100 \tag{7}$$

$$\text{Adequate precision} = \frac{max(\hat{Y}) - min(\hat{Y})}{\sqrt{\frac{p\sigma^2}{n}}} \tag{8}$$

where, in Eq. (3) – (8), *SS* represents the sum of squares, *DF* is the degree of freedom, *PRESS* represents the predicted residual error sum of squares, *SD* is the standard deviation, *CV* represents the coefficient of variation, MS_e is the residual mean square, *Y* represents the observed response, $\hat{Y}$ is the predicted response, *p* represents the number of model variables, σ^2 is the residual mean square from ANOVA table and *n* represents the number of experimental runs. The analyses were done with Design-Expert software package, version 10 (USA).

2.3. Moringa oil extraction procedure

The established technique earlier described by Akintunde et al. (2015) was applied for this present study. Solvent extraction technique using a Soxhlet apparatus connected to a condenser and a 250-ml round-bottom flask was employed. Oil extraction capability of three different solvents: ethyl acetate, ethanol and *n*-hexane, were examined. Relevant properties of the selected solvents for the extraction studies are shown in Table 2. According to the different set of extraction conditions generated in the experimental design (Table 3), specified quantity of the pulverized *Moringa* kernels wrapped in a muslin fabric was firstly placed in the thimble of the extractor. The flask was filled with 200 ml of solvent of extraction and firmly secured to the end of the extractor. Heating was provided for the experimental setup by a regulated water bath operated at the boiling point of each of the examined solvent. At the end of each experiment, distillation method was used to recover the solvent in the oil-solvent mixture. Each experiment was carried out in duplicate and the mean with the standard deviation was calculated. The quantity of MOSO extracted was calculated according to Eq. (9).

$$\text{MOSO yield (wt. \%)} = \frac{\text{Quantity of extracted MOSO (g)}}{\text{Quantity of pulverized } Moringa \text{ kernels (g)}} \times 100 \tag{9}$$

Table 2
Relevant properties of the selected solvents for the extraction studies.

Properties	*n*-hexane	ethyl acetate	ethanol
Type of solvent	non-polar	polar	polar
Category of solvent	Hydrocarbon	ester	alcohol
Dielectric constant	1.9	6.0	24.5
Dipole moment	0.08	1.88	1.66
Polarity index	0.1	4.4	5.2
Boiling point (°C)	68.7	77.1	78.3
Melting Point (°C)	−96.0	−83.6	−114.14
Flash point (°C)	−26.0	−4.0	16.60
Density (g/cm^3)	0.6606	0.902	0.7893
Molar mass (g/mol)	86.18	88.11	46.07
Viscosity (cP)	0.29	0.43	1.074
Cost ($)/per litre	5.50	4.40	4.40

The MOSO obtained was stored in corked containers until further analysis.

2.3.1. Characteristics of MOSO

To characterize the extracted MOSO samples, physical properties such as refractive index, kinematic viscosity and density; and chemical properties such as iodine value, peroxide value, saponification value, acid value and free fatty acid (% FFA) content, were all determined using the standard analytical methods of AOAC (1990). The physical state and color of MOSO samples were done by visual inspection and compared with standard colors in an ambient light source. Functional group analysis by Fourier transform infrared (FT-IR) and fatty acid compositions of the MOSO by gas chromatography (GC) were carried out as earlier described in our previous work (Okeleye and Betiku, 2019).

The oxidative stability index (OSI) method was used to measure the oxidative stability based on the induction period. This was done using the empirical correlation between OSI and bis-allylic position equivalents (BAPE) developed by Knothe and Dunn (2003):

Table 3
Design matrix with observed and predicted MOSO yields.

Run	Quantitative variables		Qualitative variable	MOSO yield (wt.%)	
	Solid/ solvent ratio (g/ml)	Extraction time (h)	Solvent type	Observed	Predicted
1	0.050	1	*n*-hexane	27.60 ± 0.03	27.58
2	0.050	1	*n*-hexane	27.55 ± 0.07	27.58
3	0.200	1	*n*-hexane	8.20 ± 0.18	8.06
4	0.200	1	*n*-hexane	8.22 ± 0.10	8.06
5	0.125	2	*n*-hexane	22.00 ± 0.11	22.62
6	0.050	3	*n*-hexane	41.50 ± 0.18	41.60
7	0.050	3	*n*-hexane	42.00 ± 0.00	41.60
8	0.050	1	ethyl acetate	10.45 ± 0.42	10.72
9	0.050	1	ethyl acetate	10.50 ± 0.18	10.72
10	0.200	1	ethyl acetate	3.00 ± 0.08	2.75
11	0.125	1.5	ethyl acetate	6.04 ± 0.11	5.71
12	0.050	3	ethyl acetate	14.15 ± 0.02	14.05
13	0.050	3	ethyl acetate	14.28 ± 0.22	14.05
14	0.200	3	ethyl acetate	3.40 ± 0.02	3.62
15	0.200	3	ethyl acetate	3.43 ± 0.10	3.62
16	0.050	1	ethanol	7.35 ± 0.00	6.99
17	0.125	1	ethanol	3.60 ± 0.01	3.50
18	0.200	1	ethanol	2.20 ± 0.00	2.85
19	0.050	2	ethanol	7.84 ± 0.02	7.74
20	0.125	2	ethanol	3.88 ± 0.11	3.64
21	0.200	2	ethanol	2.40 ± 0.02	2.37
22	0.050	3	ethanol	8.24 ± 0.00	8.85
23	0.125	3	ethanol	4.08 ± 0.10	4.13
24	0.200	3	ethanol	2.73 ± 0.01	2.25

Actual MOSO yields are mean ± standard deviation of duplicate runs.

Table 4
Analysis of variance (ANOVA) results for the regression model of MOSO extraction.

Source of variance	Sum of Squares	DF	Mean Square	F-value	p-value	Quality of fit and statistical indices	
						Parameter	Value
Model	3186.21	11	289.66	1527.22	< 0.0001[a]	R^2	0.9993
A-Solid/solvent ratio	468.12	1	468.12	2468.20	< 0.0001[a]	Adjusted R^2	0.9986
B-Extraction time	89.92	1	89.92	474.13	< 0.0001[a]	Predicted R^2	0.9965
C-Solvent type	1508.72	2	754.36	3977.41	< 0.0001[a]	Adequate Precision	127.761
AB	4.21	1	4.21	22.19	0.0005[a]	Standard Deviation	0.44
AC	122.88	2	61.44	323.96	< 0.0001[a]	Mean	11.86
BC	85.06	2	42.53	224.24	< 0.0001[a]	% CV	3.67
A^2	6.03	1	6.03	31.77	0.0001[a]	PRESS	11.04
B^2	0.085	1	0.085	0.45	0.5148		
Residual	2.28	12	0.19				
Lack-of-Fit	2.14	6	0.36	15.66	0.0020		
Pure Error	0.14	6	0.023				
Corrected Total SS	3188.49	23					

[a] Statistically significant at the confidence level of 95%, DF – degree of freedom, CV – coefficient of variation, PRESS – predicted residual error sum of squares, SS – sum of squares.

$$\text{BAPE} = \%\,\text{C18:2} + (2 \times \%\,\text{C18:3}) \tag{10}$$

$$\text{OSI} = 3.91 - 0.045 \times \text{BAPE} \tag{11}$$

where, % C18:2 and % C18:3 are the percentage amounts of linoleic and linolenic acids content, respectively.

3. Results and discussion

3.1. Multiple regression equation model

For the prediction of MOSO yield at 95% confidence level, the numerical values of coefficients estimated for the linear, cross-product (interactive) and quadratic expression of the variables are presented in terms of mathematical equation of actual factors. The best fit quadratic model equation expressed in terms of coded factors in Eq. (12) – (14) can be used to make predictions about the desired response at any given level of each process variable.

For *n*-hexane:

$$Y = 29.71426–0.92453A + 6.70808B–0.040991\text{AB} + 0.00629773\text{A}^2 + 0.17808B^2 \tag{12}$$

For ethyl acetate:

$$Y = 14.35802–0.53955A + 1.36161B–0.040991\text{AB} + 0.00629773A^2 + 0.17808B^2 \tag{13}$$

For ethanol:

$$Y = 10.07657–0.41179A + 0.62913B–0.040991\text{AB} + 0.00629773A^2 + 0.17808B^2 \tag{14}$$

where, *Y* is the MOSO yield (wt. %), *A* is the solid/solvent ratio (g/ml) and *B* is the extraction time (h).

3.2. Results of statistical analysis of model

The experimental matrix obtained from the D-optimal design along with the observed and predicted MOSO yield are depicted in Table 3. High F-value (1527.22) and low p-value (< 0.0001) obtained in this study demonstrate significance of the developed quadratic regression model (Table 4). The ANOVA results observed in this study show that all the terms of the regession model are significant, i.e. $p < 0.05$, but one. The linear terms of the solid/solvent ratio (*A*), extraction time (*B*) and solvent type (*C*) are all significant. Similarly, the three interactive terms and quadratic term of solid/solvent ratio are all significant at 95% confidence level. However, the quadratic term of extraction time is insignificant. The relative level of importance of the model is shown in Fig. 1. Solvent type (qualitative variable) exerted the most influence on the MOSO yield and next in line solid/solvent ratio (quantitative variable) and then, the extraction time (quantitative variable) (Table 4 and Fig. 1).

The characteristics of the fitted regression model was examined using R^2, adjusted R^2 and predicted R^2 (Table 4). High R^2 value of 0.9993 indicates that 99.93% variation of the quadratic model could be accounted for by the model regression equation. This was corroborated by the reasonable agreement between the predicted R^2 (0.9965) and adjusted R^2 (0.9986) of the quadratic model (Myers et al., 2009). The statistical significance of the regression model was also established by the low values of SD (0.44) and CV (3.67%) of the experimental data.

3.3. Model adequacy test

The adequacy of the model was checked through diagnostic plots (Fig. 2). Parity plot of predicted MOSO yield versus observed (experimental) MOSO yield is depicted in Fig. 2a, which shows that the predicted responses by the model equations agrees with the observed responses as fitted points lie closely along a straight line. Fig. 2b displays the normal plot of residuals. The plot shows no obvious challenge with normality since the residuals plot approximate on a straight line, which satisfied the normality assumption. The plot of studentized residuals against predicted MOSO yield is illustrated in Fig. 2c. From the plot, the residuals arbitrarily scattered indicating that the variance of the original observations is constant for the response of each run. The plot of

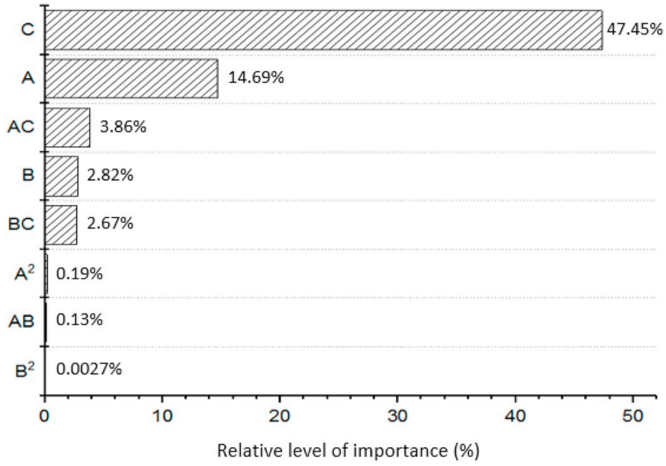

Fig. 1. Relative level of importance of process input variables on MOSO yield.

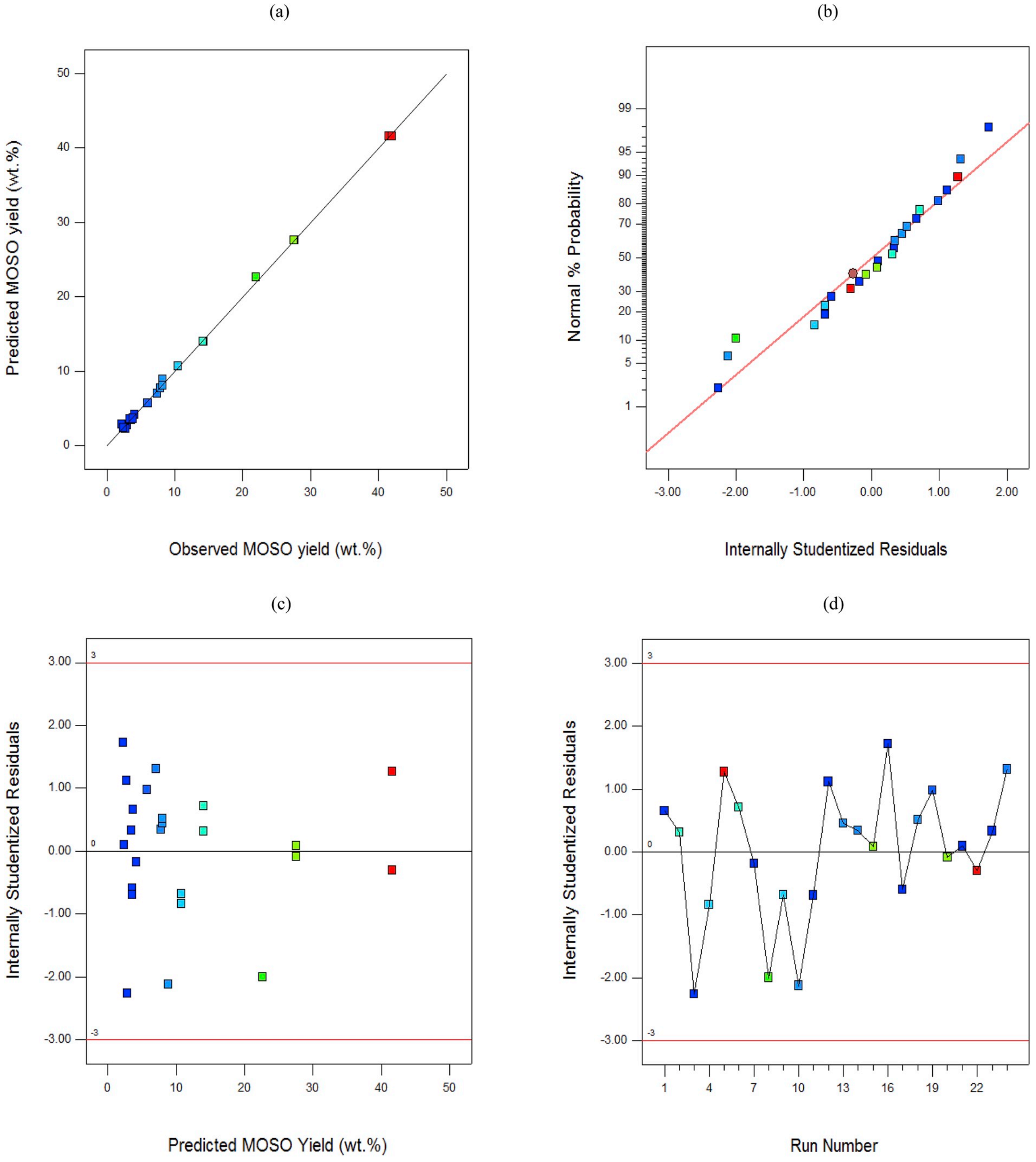

Fig. 2. Model adequacy plots of MOSO extraction. (a) predicted yield *vs.* observed yield; (b) normal plot of residuals; (c) residuals *vs.* predicted and (d) outlier *t* plot.

residuals versus experimental run of MOSO is presented in Fig. 2d. The residuals should lie within -3.00 to +3.00 interval. No data was outside the range demonstrating that the fitted model to the response surface was consistent with all the data, which confirms no error in recording of the data (Noshadi et al., 2012).

3.4. Effect of extraction process variables on MOSO yield

3.4.1. Quantitative interaction of extraction variables on MOSO yield

Fig. 3 (a–c) shows the contour and surface plots effect of the solid/solvent ratio and extraction time on MOSO yield using *n*-hexane, ethyl acetate and ethanol as solvents of extraction, respectively. The figures show that the solid/solvent ratio, extraction time as well as their interaction follow a directly proportional relationship i.e. for all the solvents of extraction considered, the MOSO yield increases as the extraction time increases. With *n*-hexane, maximum experimental MOSO yield of 42.00 wt% was observed under the condition of extraction time of 3 h and solid/solvent ratio of 0.05 g/ml, while under the same extraction conditions, MOSO yield of 8.24 and 14.28 wt% could be achieved using ethanol and ethyl acetate as solvents of extraction, respectively. This observation could be due to adequate mass transfer between the solid (pulverized *Moringa* seeds) and the solvents of extraction, leading to opening of cell walls to allow more extraction of oil from the pores of the pulverized seed. Low solid/solvent ratio allows further diffusion of the solvent through the pores of the pulverized seeds, thus, influencing more extraction of oil. This relationship

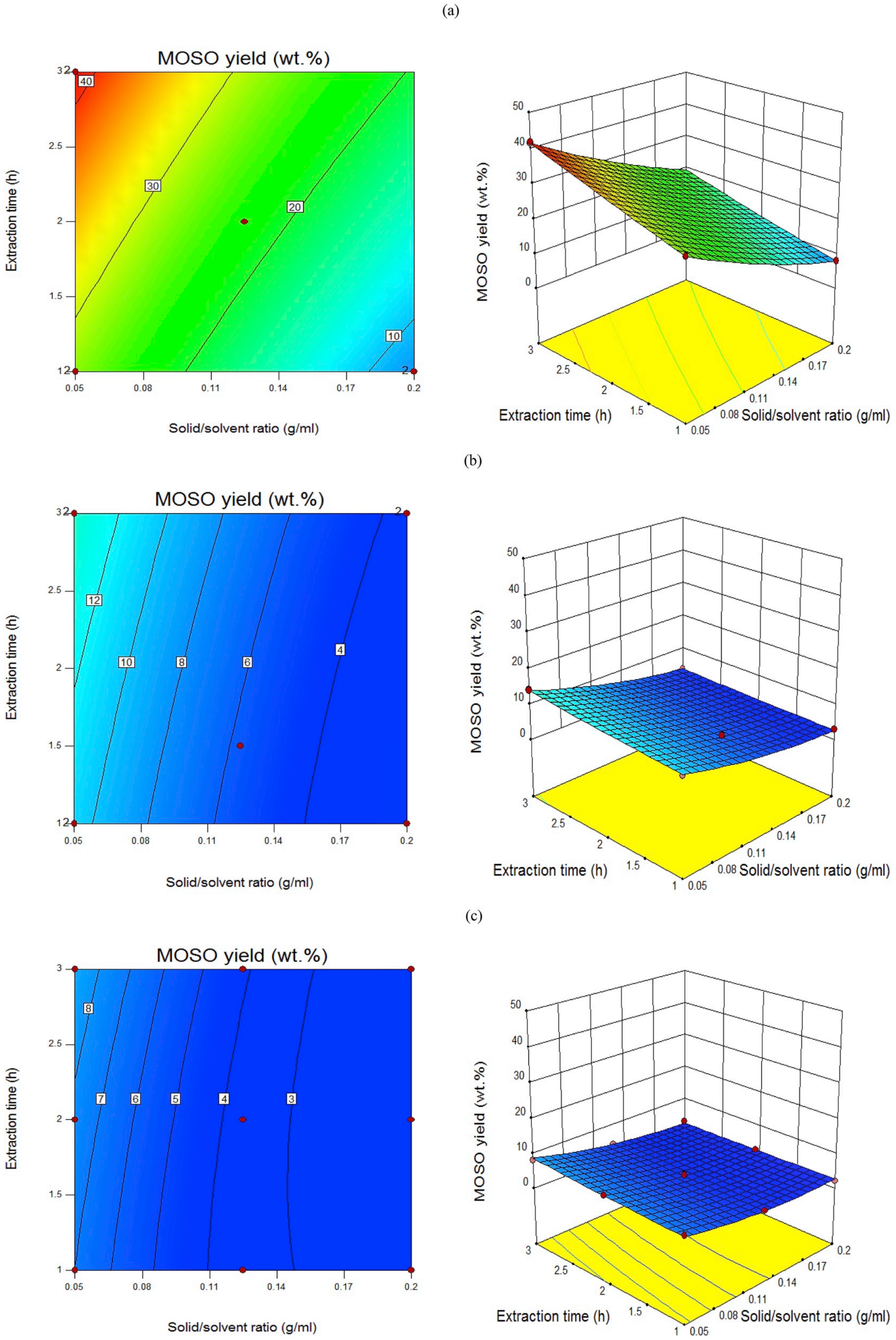

Fig. 3. Contour and surface plots of the effect of extraction time and solid/solvent ratio on MOSO yield using (a) *n*-hexane; (b) ethyl acetate and (c) ethanol.

between the solid/solvent ratio and oil yield has been reported in the extraction of yellow oleander seed oil with petroleum ether (Ajala and Betiku, 2015) and also on the work done on *Kariya* seed oil using acetone, *n*-hexane and ethyl acetate (Okeleye and Betiku, 2019).

3.4.2. Qualitative effect of solvent of extraction properties on MOSO yield

The most influential variable on the MOSO yield was solvent type. The MOSO yield increased significantly from ethanol to ethyl acetate, and finally to *n*-hexane. Based on properties of the selected solvents of

Table 5

Properties of solvent extracted MOSO in this work in comparison with literature reports.

Property	*n*-hexane	Mean values This study	ethanol	Tsaknis et al. (1998) [a]	Anwar and Bhanger (2003) [a]	Rahman et al. (2009) [a]	Ruttarattanamongkol et al. (2014) [a]
		ethyl acetate Nigeria[b]		*n*-hexane Malawi[b]	*n*-hexane Pakistan[b]	LPE Bangladesh[b]	LPE Thailand[b]
Physical state and color at 25 °C	Liquid/clear/corn-yellow	Liquid/clear/amber-yellow	Liquid/cloudy/off-black	Liquid/clear/pale yellow	NS	NS	Liquid/clear/bright yellow
Oil yield (wt.%)	41.71 ± 0.00	14.28 ± 0.22	8.24 ± 0.00	35.3	40.39	35.6	ND
Refractive index at 40 °C	1.458 ± 0.00	1.459 ± 0.00	1.456 ± 0.00	1.4559	1.4608	1.457	ND
Density (kg/m^3) at 25 °C	903.00 ± 0.02	911.00 ± 0.01	933.00 ± 0.01	888.2	905.7	892.0	ND
Kinematic viscosity at 40 °C (mm^2/s)	60.04 ± 0.43	49.73 ± 0.47	40.10 ± 1.13	62	ND	59.5	ND
Acid value (mg KOH/g oil)	2.88 ± 0.07	3.40 ± 0.04	8.25 ± 0.01	ND	ND	ND	ND
% FFA	1.44 ± 0.03	1.71 ± 0.02	4.15 ± 0.00	0.82	0.40	1.14	1.72
Saponification value (mg KOH/g oil)	177.65 ± 2.14	187.47 ± 1.62	174.88 ± 0.81	184.16	186.67	178	124.2
Iodine value (g I$_2$/100 g oil)	65.89 ± 0.49	79.23 ± 0.75	75.98 ± 0.64	65.74	69.45	66.9	68.59
Peroxide value (meq O$_2$/kg oil)	1.25 ± 0.36	1.80 ± 0.34	2.20 ± 0.38	0.23	0.59	0.87	1.01
Oxidative stability (h)	3.87	3.87	3.89	23.7[c]	8.63[c]	14.4[c]	ND

[a] Average values of the seed oil data reported.

[b] Country of oilseeds origin.

[c] Rancimat method at 120 °C, LPE – light petroleum ether, NS – not stated, ND – not determined.

extraction, it was observed that as polarity of solvent of extraction decreases, MOSO yield increases. The high yield obtained with *n*-hexane may be due to its polarity index and boiling point which are lower than that of ethyl acetate and ethanol, thereby causing the *n*-hexane molecules to travel faster through the pulverized kernels (Yang et al., 2014). The solubility of ethyl acetate and ethanol as polar solvents could have been negatively affected by the non-polar groups (i.e. fatty acid chains) of the triglycerides, therefore, leading to lower oil yield compared to *n*-hexane (a non-polar solvent). Furthermore, the high yield obtained with *n*-hexane may possibly due to the absence of OH group which has been reported to interfere with the extraction process of some oilseeds (Jayaprakasha et al., 2001). On the other hand, the higher polarity and dipole moment of the polar solvents (ethyl acetate and ethanol) could have limited the solubility of the lipids, leading to hydrolysis of some lipids (Russin et al., 2011), thus, resulting in lower oil yield. Oil yield and properties of the extracted MOSO samples in comparison with some literature reports are presented in Table 5. The variations in oil yield across habitat may be due to the diversity of geological, natural habitats, agro-climatic and environmental conditions of the countries as well as the solvents of extraction used (Anwar and Rashid, 2007).

3.5. *Optimization result of MOSO extraction process*

The established best operating condition for the process was solid/solvent ratio of 0.05 g/ml and extraction time of 3 h using *n*-hexane with a predicted MOSO yield of 41.60 wt%. After the optimal condition was confirmed experimentally in the laboratory using the optimal condition three times, an average of 41.72 ± 0.45 wt% MOSO yield was obtained, which confirms the efficiency of the model developed in illustrating the process of MOSO extraction. It is noteworthy in earlier studies (Mani et al., 2007; Abdulkareem et al., 2011), the time of extraction used was more than double the 3 h obtained in this present work.

3.6. *Characterization of extracted MOSO samples*

3.6.1. *Results of physicochemical analysis of extracted MOSO samples*

The physicochemical properties of the MOSO samples extracted using *n*-hexane, ethyl acetate and ethanol showed that they were affected by nature of solvent used for the extraction (Table 5). The physical state of MOSO at room temperature was liquid for all the samples. The appearance (color) was corn-yellow for *n*-hexane, amber-yellow for ethyl acetate and an off-black color for ethanol extract (Fig. 4). The dark color of MOSO samples extracted with the polar solvents (ethyl acetate and ethanol) is attributable to the existence of products from Maillard reaction in the polar lipid fractions (Ramadan et al., 2003) and the occurrence of tocopherol pigments present in the *Moringa* seeds (Bhutada et al., 2016). Polar solvents have been noted to have the capacity in dissolving glucosinolate component, some portion of the carbohydrate and phenolic contents as well as the phospholipids of oilseeds which thus, influence the appearance of extracted oil (Rubin et al., 1984). The coloring matter content of oilseeds has been reported to increase gradually with increase in dielectric constant (Attah and Ibemesi, 1990). Increase in dark appearance of the oil samples from *n*-hexane to ethanol (Fig. 4) also corresponds with increase in polarity index and dipole moment of the extraction solvents (Table 2). Variations in viscosity of the samples may be a sign of the existence of higher molecular weight materials in the extracted oil sample, especially with *n*-hexane. Except for MOSO extracted with ethanol, the acid values (AVs) are below the maximum limit of 4.0 mg KOH/g oil specified for edible oils as given by FAO/WHO (1993). AVs and % FFA contents of MOSO extracted with non-polar solvent (*n*-hexane) was lower than that of oil extracted with polar solvents (ethyl acetate and ethanol) since FFAs are more soluble in polar solvents. The saponification value of the MOSO was higher with ethyl acetate than that of *n*-hexane and ethanol (Table 5). This could be attributed to the fact that ethyl acetate, which

Fig. 4. Appearance of the extracted MOSO samples.

(a)

n-hexane

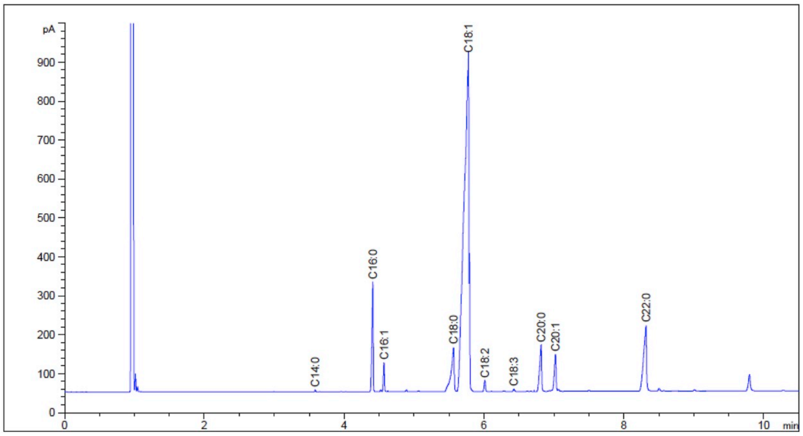

(b)

ethyl acetate

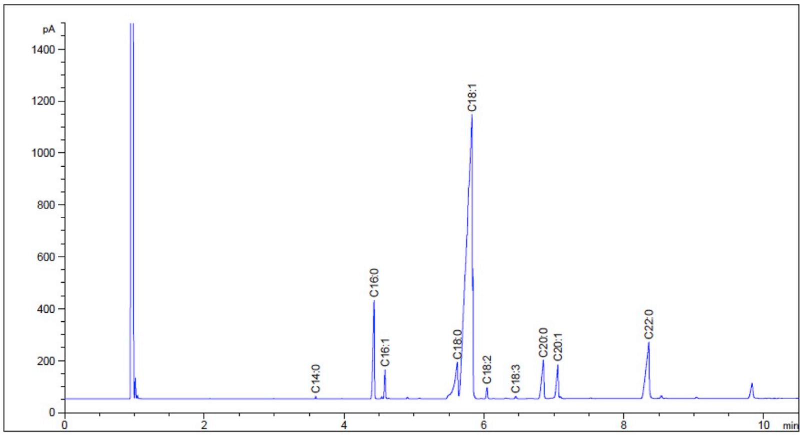

(c)

ethanol

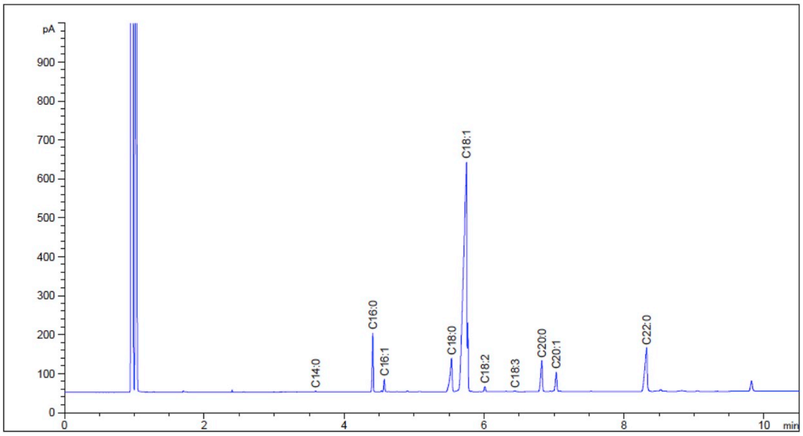

Fig. 5. Chromatograms for MOSO extracted samples.

Table 6
Fatty acid composition of solvent extracted MOSO in this study in comparison with literature values.

Fatty acid	Structure	*n*-hexane	Mean values This study	ethanol	Tsaknis et al. (1998) [a]	Anwar and Bhanger (2003) [a]	Rahman et al. (2009) [a]	Ruttarattanamongkol et al. (2014) [a]
			ethyl acetate Nigeria§		*n*-hexane Malawi§	*n*-hexane Pakistan§	LPE Bangladesh§	LPE Thailand§
Caprylic	C8:0	ND	ND	ND	0.02	ND	0.03	ND
Myristic	C14:0	0.070	0.077	0.066	0.10	ND	0.10	ND
Palmitic	C16:0	6.17	6.44	5.80	5.51	6.50	6.46	6.26
Margaric	C17:0	ND	ND	ND	0.04	ND	0.07	ND
Stearic	C18:0	5.58	5.69	6.46	5.86	5.67	5.82	6.30
Arachidic	C20:0	3.87	3.89	4.74	3.78	3.00	3.39	3.94
Behenic	C22:0	8.12	8.21	9.39	6.81	5.00	6.58	6.19
Lignoceric	C24:0	ND	ND	ND	ND	ND	ND	1.10
Cerotic	C26:0	ND	ND	ND	0.98	ND	1.12	ND
Σ Saturated		*23.81*	*24.31*	*26.46*	*23.10*	*20.17*	*23.57*	*23.80*
Palmitoleic	C16:1	1.29	1.35	1.14	1.09	1.00	1.44	1.20
Oleic	C18:1	71.31	70.65	69.00	67.79	76.00	71.30	71.49
Linoleic	C18:2	0.61	0.64	0.56	0.71	1.29	0.96	0.50
Linolenic	C18:3	0.13	0.14	0.11	0.21	ND	0.21	0.19
Gadoleic	C20:1	2.85	2.91	2.73	2.60	1.20	2.88	2.18
Erucic	C22:1	ND	ND	ND	0.11	ND	0.13	ND
Σ *Monounsaturated*		75.45	74.91	72.87	71.59	78.20	75.75	74.21
Σ *Polyunsaturated*		0.74	0.78	0.67	0.92	1.29	1.17	0.68
Σ *Unsaturated*		*76.19*	*75.69*	*73.54*	*72.51*	*79.49*	*76.92*	*74.89*

[a] Average values of the seed oil data reported, § Country of seed origin, LPE – light petroleum ether, ND – not determined.

is categorized as an ester solvent, has tendency to extract higher level of unsaponifiable lipids. The variation in iodine value of the MOSO indicates ethanol and ethyl acetate extracted some coloring matter with some level of unsaturation than *n*-hexane (Akaranta and Anusiem, 1996). Peroxide values (PVs) obtained for the oil samples are below the maximum limit of 10.0 meq O_2/kg oil stated for edible oils by FAO/WHO (1993). PV was higher for oil obtained using polar solvents. This may be due to utilization of slight amount of oxygen during autoxidation in the extraction process than that of *n*-hexane. Low PV in the oil samples show they can easily resist lipolytic hydrolysis and oxidative deterioration, and therefore, have long shelf life, with *n*-hexane extracted having the highest resistance. The OSI values of the MOSO samples were calculated to be ~3.9 h for the three solvents of extraction. Low induction period values obtained proves the good oxidative stability of the MOSO samples, thus, results in a good storage attribute of the MOSO. The characteristic of the MOSO in this work compared reasonably well with literature values (Table 5).

3.6.2. GC analysis results of MOSO samples

The chromatograms obtained for the MOSO samples are displayed in Fig. 5a–c. Table 6 displays the prominent fatty acids in all the extracted MOSO samples in comparison with reported literature values. The unsaturated fatty acids fraction was higher than the saturated fatty acids fraction in all the MOSO samples obtained in this study. Fatty acid compositions were 73.54, 75.69 and 76.19% for unsaturated fractions and 26.46, 24.31 and 23.81% for saturated fractions using ethanol, ethyl acetate and *n*-hexane, respectively. The high oleic acid content of the MOSO gives the oil an advantage over other oils such palm oil, soybean oil and canola oil when used in frying due to its stability (Nguyen et al., 2011).

3.6.3. Spectral analysis results

FT-IR spectra for the extracted MOSO samples are shown in Fig. 6a–c and Table 7 illustrates the characteristics of the peaks from the spectra. Comparable peaks are observed in all the spectra, implying that the choice of solvent had no effect on the functional groups of the MOSO samples. Overtone of glyceride ester carbonyl absorption is located as weak peak at 3468 cm^{-1}. The presence of symmetric and asymmetric stretching vibrations of –C–H in CH_2 group is corroborated by occurrence of very strong peaks located at 2854 and 2924 cm^{-1}, respectively (Coates, 2000). The very weak band in the range 2730–2677 cm^{-1} is probably due to Fermi resonance of the carbonyl group. Occurrence of C=O group of triglycerides in the three samples, is attributed to a stretching vibration of two strong bands detected at 1745 and 1747 cm^{-1}, respectively. The C=C stretching mode of unconjugated olefins displays very weak peaks present at band range 1667–1640 cm^{-1} (Silverstein et al., 2014). Peaks at 1238, 1163 and 1097 cm^{-1} within the fingerprint region, could all be assigned to the stretching vibrations of the C–O group in esters in all samples. Also, peak at 1238 and 1163 cm^{-1} are ascribed to the bending vibration out-of-plane of the methylene group (Silverstein et al., 2014).

4. Conclusion

There is renewed interest in modern utilization of vegetable oils to meet the rising needs on food and energy in the world. *Moringa oleifera* seed oil extraction using solvent extraction method was modeled and optimized in this work using D-optimal design. Effect of process variables namely, extraction time, type of solvent and solid/solvent ratio on oil yield were investigated. The quadratic model best described the extraction process and the process variables considered were found to be statistically significant. An optimum average yield of 41.72 ± 0.45 wt% was obtained using 0.05 g/ml of solid/solvent ratio and 3 h extraction time with *n*-hexane. Characterization of the extracted MOSO revealed that nature of solvent used had influence on its color and some properties. While the oil yield was dependent on the solvent of extraction, the FT-IR spectra reveal no significant changes in the functional groups present. However, the GC analysis showed slight variations in the fatty acid profile of the MOSO samples. Thus, if cultivated on a large scale, *M. oleifera* can be regarded as a substitute source of vegetable oil for various purposes.

(a)

n-hexane

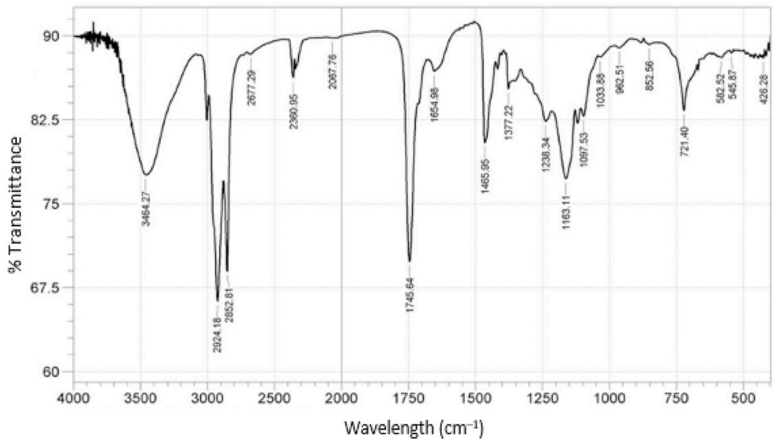

(b)

ethyl acetate

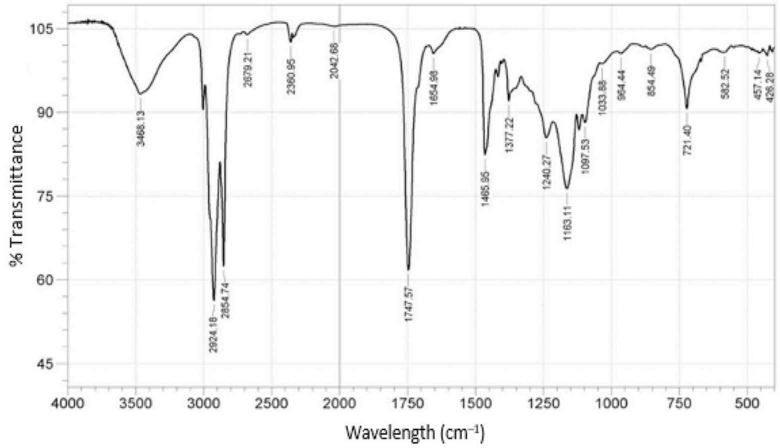

(c)

ethanol

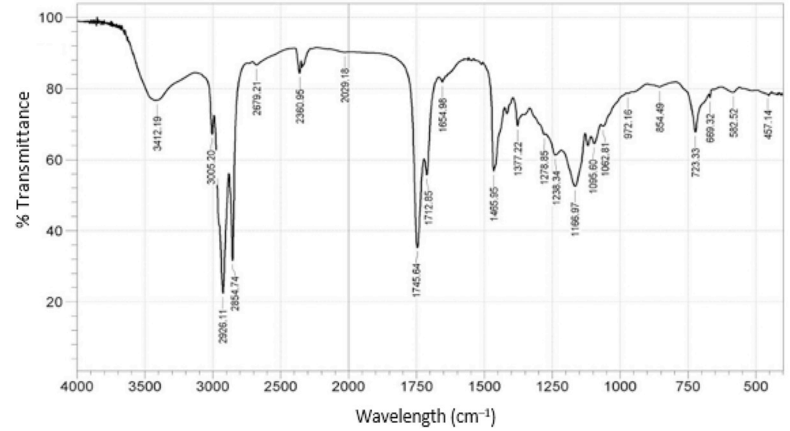

Fig. 6. FT-IR spectra for MOSO extracted samples.

Table 7
Properties of absorption peaks detected in the FT-IR spectra of extracted MOSO samples.

Range, cm^{-1}	Nominal frequency			Functional group	Mode of vibration	Intensity
	n-hexane	ethyl acetate	ethanol			
3550–3220	3464.27	3468.13	3412.19	–C=O (ester)	overtone	weak
2946–2881	2924.18	2924.18	2926.11	–C–H (CH_2)	stretching (asymmetric)	very strong
2881–2782	2852.81	2854.74	2854.74	–C–H (CH_2)	stretching (symmetric)	very strong
2730–2677	2677.29	2679.21	2679.21	–C=O (ester)	Fermi resonance	very weak
1795–1677	1745.64	1747.57	1745.64	–C=O (ester)	stretching	very strong
1667–1640	1654.98	1654.96	1654.96	–C=C– (*cis*)	stretching	very weak
1486–1446	1465.95	1465.95	1465.95	–C–H (CH_2)	bending (scissoring)	medium
1382–1371	1377.22	1377.22	1377.22	–C–H (CH_3)	bending (symmetric)	medium
1290–1211	1238.34	1240.27	1238.34	–C–O, –CH_2–	stretching, bending (out-of-plane)	medium
1211–1147	1163.11	1163.11	1166.97	–C–O, –CH_2–	stretching, bending	strong
1106–1072	1097.53	1097.53	1095.60	–C–O	stretching	medium
1006–929	962.51	964.44	972.16	–HC=CH– (*trans*)	bending (out-of-plane)	very weak
885–802	852.56	854.49	854.49	= CH_2	wagging	very weak
754–701	721.40	721.40	723.33	–$(CH_2)_n$–, –HC=CH– (*cis*)	rocking, bending (out-of-plane)	medium

Conflicts of interest

We declare no conflict of interest.

Acknowledgement

Authors acknowledge the technical assistance provided by A. A. Okeleye.

Appendix A. Supplementary data

Supplementary data to this article can be found online at https://doi.org/10.1016/j.bcab.2019.101187.

References

Abdulkareem, A., Uthman, H., Afolabi, A.S., Awenebe, O., 2011. Extraction and Optimization of Oil from *Moringa Oleifera* Seed as an Alternative Feedstock for the Production of Biodiesel, Sustainable Growth and Applications in Renewable Energy Sources. IntechOpen.

Abdulkarim, S., Long, K., Lai, O.M., Muhammad, S., Ghazali, H., 2007. Frying quality and stability of high-oleic *Moringa oleifera* seed oil in comparison with other vegetable oils. Food Chem. 105, 1382–1389.

Ajala, S.O., Betiku, E., 2015. Yellow oleander seed oil extraction modeling and process parameters optimization: performance evaluation of artificial neural network and response surface methodology. J. Food Process. Preserv. 39, 1466–1474.

Akaranta, O., Anusiem, A., 1996. A bioresource solvent for extraction of castor oil. Ind. Crops Prod. 5, 273–277.

Akintunde, A.M., Ajala, S.O., Betiku, E., 2015. Optimization of *Bauhinia monandra* seed oil extraction via artificial neural network and response surface methodology: a potential biofuel candidate. Ind. Crops Prod. 67, 387–394.

Anwar, F., Bhanger, M., 2003. Analytical characterization of *Moringa oleifera* seed oil grown in temperate regions of Pakistan. J. Agric. Food Chem. 51, 6558–6563.

Anwar, F., Rashid, U., 2007. Physico-chemical characteristics of *Moringa oleifera* seeds and seed oil from a wild provenance of Pakistan. Pakistan J. Bot. 39, 1443–1453.

AOAC, 1990. Official Methods of Analysis of the Association of the Official Analytical Chemists. AOAC, Washington, VA/U.S.A.

Attah, J., Ibemesi, J., 1990. Solvent extraction of the oils of rubber, melon, pumpkin and oilbean seeds. J. Am. Oil Chem. Soc. 67, 25–27.

Bargale, P., Ford, R., Sosulski, F., Wulfsohn, D., Irudayaraj, J., 1999. Mechanical oil expression from extruded soybean samples. J. Am. Oil Chem. Soc. 76, 223–229.

Bhatnagar, A.S., Krishna, A.G.G., 2013. Effect of extraction solvent on oil and bioactives composition of commercial Indian Niger (*Guizotia abyssinica* (Lf) Cass.) seed. J. Am. Oil Chem. Soc. 90, 1203–1212.

Bhutada, P.R., Jadhav, A.J., Pinjari, D.V., Nemade, P.R., Jain, R.D., 2016. Solvent assisted extraction of oil from *Moringa oleifera* Lam. seeds. Ind. Crops Prod. 82, 74–80.

Coates, J., 2000. Interpretation of infrared spectra, a practical approach. In: Meyers, R.A. (Ed.), Encyclopedia of Analytical Chemistry. John Wiley & Sons Ltd, Chichester.

Dunford, N.T., Zhang, M., 2003. Pressurized solvent extraction of wheat germ oil. Food Res. Int. 36, 905–909.

Elsayed, E.A., Sharaf-Eldin, M.A., Wadaan, M., 2015. In vitro evaluation of cytotoxic activities of essential oil from *Moringa oleifera* seeds on HeLa, HepG2, MCF-7, CACO-2 and L929 cell lines. Asian Pac. J. Cancer Prev. APJCP 16, 4671–4675.

FAO/WHO, 1993. Report of the 14th Session of the Codex Alimentarius Committee on Fats and Oils. 27 September - 1 October 1993. FAO, London, United Kingdom.

Ibrahim, A.P., Omilakin, R.O., Betiku, E., 2019. Optimization of microwave-assisted solvent extraction of non-edible sandbox (*Hura crepitans*) seed oil: a potential biodiesel feedstock. Renew. Energy 141, 349–358.

Jayaprakasha, G., Singh, R., Sakariah, K., 2001. Antioxidant activity of grape seed (*Vitis vinifera*) extracts on peroxidation models in vitro. Food Chem. 73, 285–290.

Kittiphoom, S., Sutasinee, S., 2013. Mango seed kernel oil and its physicochemical properties. International Food Research Journal 20, 1145.

Knothe, G., Dunn, R.O., 2003. Dependence of oil stability index of fatty compounds on their structure and concentration and presence of metals. J. Am. Oil Chem. Soc. 80, 1021–1026.

Latif, S., Anwar, F., 2011. Aqueous enzymatic sesame oil and protein extraction. Food Chem. 125, 679–684.

Lohani, U.C., Fallahi, P., Muthukumarappan, K., 2015. Comparison of ethyl acetate with hexane for oil extraction from various oilseeds. J. Am. Oil Chem. Soc. 92, 743–754.

Mahmood, K.T., Mugal, T., Haq, I.U.l., 2010. *Moringa oleifera*: a natural gift-A review. J. Pharm. Sci. Res. 2, 775–781.

Mani, S., Jaya, S., Vadivambal, R., 2007. Optimization of solvent extraction of moringa (*Moringa oleifera*) seed kernel oil using response surface methodology. Food Bioprod. Process. 85, 328–335.

Myers, R.H., Montgomery, D.C., Anderson-Cook, C., 2009. Response Surface Methodology: Product and Process Optimization Using Designed Experiments. John Wiley & Sons, New York.

Nguyen, H.N., Pag-asa, D.G., Maridable, J.B., Malaluan, R.M., Hinode, H., Salim, C., Huynh, H.K.P., 2011. Extraction of oil from *Moringa oleifera* kernels using supercritical carbon dioxide with ethanol for pretreatment: optimization of the extraction process. Chem. Eng. Process: Process Intensification 50, 1207–1213.

Noshadi, I., Amin, N., Parnas, R.S., 2012. Continuous production of biodiesel from waste cooking oil in a reactive distillation column catalyzed by solid heteropolyacid: optimization using response surface methodology (RSM). Fuel 94, 156–164.

Okeleye, A.A., Betiku, E., 2019. Kariya (*Hildegardia barteri*) seed oil extraction: comparative evaluation of solvents, modeling, and optimization techniques. Chem. Eng. Commun. 206, 1181–1198.

Pradhan, R.C., Meda, V., Rout, P.K., Naik, S., Dalai, A.K., 2010. Supercritical CO2 extraction of fatty oil from flaxseed and comparison with screw press expression and solvent extraction processes. J. Food Eng. 98, 393–397.

Rahman, I.M., Barua, S., Nazimuddin, M., Begum, Z.A., Rahman, M.A., Hasegawa, H., 2009. Physicochemical properties of *Moringa oleifera* lam. Seed oil of the indigenous-cultivar of Bangladesh. J. Food Lipids 16, 540–553.

Ramadan, M.F., Kroh, L.W., Mörsel, J.-T., 2003. Radical scavenging activity of black cumin (*Nigella sativa* L.), coriander (*Coriandrum sativum* L.), and Niger (*Guizotia abyssinica* Cass.) crude seed oils and oil fractions. J. Agric. Food Chem. 51, 6961–6969.

Rashid, U., Anwar, F., Ashraf, M., Saleem, M., Yusup, S., 2011. Application of response surface methodology for optimizing transesterification of *Moringa oleifera* oil: biodiesel production. Energy Convers. Manag. 52, 3034–3042.

Rubin, L.J., Diosady, L.L., Phillips, C.R., 1984. Solvent extraction of oil bearing seeds (United States Patent). Patent Number: 4460504. https://patentimages.storage.googleapis.com/61/62/7b/129ff887964272/US4460504.pdf.

Russin, T.A., Boye, J.I., Arcand, Y., Rajamohamed, S.H., 2011. Alternative techniques for defatting soy: a practical review. Food Bioprocess Technol. 4, 200–223.

Ruttarattanamongkol, K., Siebenhandl-Ehn, S., Schreiner, M., Petrasch, A.M., 2014. Pilot-scale supercritical carbon dioxide extraction, physico-chemical properties and profile characterization of Moringa oleifera seed oil in comparison with conventional extraction methods. Ind. Crops Prod. 58, 68–77.

Silverstein, R.M., Webster, F.X., Kiemle, D.J., Bryce, D.L., 2014. Spectrometric Identification of Organic Compounds. John wiley & sons.

Taghvaei, M., Jafari, S.M., Assadpoor, E., Nowrouzieh, S., Alishah, O., 2014. Optimization of microwave-assisted extraction of cottonseed oil and evaluation of its oxidative stability and physicochemical properties. Food Chem. 160, 90–97.

Tian, Y., Xu, Z., Zheng, B., Lo, Y.M., 2013. Optimization of ultrasonic-assisted extraction of pomegranate (*Punica granatum* L.) seed oil. Ultrason. Sonochem. 20, 202–208.

Tsaknis, J., Lalas, S., Gergis, V., Spiliotis, V., 1998. A total characterisation of Moringa oleifera Malawi seed oil. Riv. Ital. Sostanze Grasse 75, 21–28.

Yang, X., Lyu, H., Chen, K., Zhu, X., Zhang, S., Chen, J., 2014. Selective extraction of bio-oil from hydrothermal liquefaction of *Salix psammophila* by organic solvents with different polarities through multistep extraction separation. BioResources 9, 5219–5233.

Zhong, J., Wang, Y., Yang, R., Liu, X., Yang, Q., Qin, X., 2018. The application of ultrasound and microwave to increase oil extraction from *Moringa oleifera* seeds. Ind. Crops Prod. 120, 1–10.